CHAPTER ONE HUNDRED FORTY TWO

MECHANISM OF BEACH PROFILE DEFORMATION DUE TO ON-OFFSHORE SAND DRIFT

BY

Wi-Gwang Pae[1) and Yuichi Iwagaki M. ASCE[2)

ABSTRACT

In the present study, two-dimensional laboratory experiments were performed to investigate the sediment transport due to waves on a fixed sloping beach. Polystyrene particles and glass balls were used as tracers to determine the mass transport velocity near the bottom and the net transport velocity of sediment moving on an impermeable slope. Relationships between the mass transport velocity of water and the net sediment transport velocity are investigated experimentally. The mechanism of two-dimensional beach deformation from an initial uniform slope toward an equilibrium profile due to bed-load movement is discussed on the basis of spatial distributions of the net sediment transport velocity. In addition, some results of experiments using a movable bed are presented to confirm the validity of a beach deformation model derived from the discussion of the tracer experiments.

1. INTRODUCTION

Hydraulic characteristics in the on-offshore direction on a beach are very complicated; fluid forces which cause sediments to move vary with time, and the direction of the net transport velocity of water (mass transport velocity) is spatially changed. Moreover, the value of the mass transport velocity is dependent upon both space and time. Owing to these complexities in the hydraulic characteristics on the beach, the mechanism of sediment transport in the on-offshore direction due to waves is not so easy to understand as that in the longshore direction.

In general, the beach profile deformation is caused by the spatial difference of the net transport rate of the bottom sediment. When the net transport rate of the bottom sediment is spatially uniform, the bottom configuration does not change even if the instantaneous velocity of water particles is large. In this study, a model of the beach profile

1) M. Eng., Postgraduate, Dept. of Civil Eng., Kyoto University, Kyoto 606, Japan
2) Dr. Eng., Professor, Dept. of Civil Eng., Kyoto University, Kyoto 606 Japan

deformation is presented on the basis of the spatial distribution of the net transport velocity of bottom sediments.

Stokes (1847) is the first one who pointed out that a steady second order drift velocity (mass transport velocity) exists in an inviscid irrotational wave field. Longuet-Higgins (1953) treated the problem on the mass transport in a finite-length channel with due consideration of fluid viscosity. In his solution, the whole flow field was divided into three regions; the interior, the surface, and the bottom boundary layers. The boundary conditions are no-slip at the bottom, zero-stress on the surface, and zero net mass transport in the whole field. In the bottom boundary layer, the mass transport velocity is given as the sum of both the second order Eulerian mass transport velocity and the Lagrangian drift resulting from the first order irrotational motion inside the boundary layer. In the interior region, the mass transport velocity is derived by using the classical matching principles of standard boundary layer problem ; that is, the limit value of the boundary layer solution equals the boundary value of the interior solution.

The mass transport velocity on a sloping beach is considered to play an important role in the transport of bottom sediments. Bijker, Kalkwijk and Pieters (1974) modified Longuet-Higgins' solution in the uniform depth by incorporating the shoaling effect. The theoretical values, however, are found to be considerably larger than those obtained in their experiments. Wang, Sunamura and Hwang (1982) investigated the drift velocity at the breaking point under different types of breaking waves on a rigid, plane beach. According to their results, independently of breaker types, the drift velocity profile at the breaking point is similar to that of Longuet-Higgins, but the offshore drift velocity in the main flow column shows a more uniform vertical distribution than that in the offshore region. Iwagaki, Pae and Moriguchi (1982) investigated the net transport velocity of solid particles on a smooth sloping beach to determine the relationship between the mass transport velocity of water and the net transport velocity of bottom sediments. Their experimental results show that there are distinct correlations between the net transport velocities of glass balls and of polystyrene particles for the regions shoreward and seaward of the breaking point.

2. EXPERIMENTAL APPARATUS AND PROCEDURE

2.1 Experimental Apparatus

The wave tank used is 30 m long, 50 cm wide, and 75 cm deep. One side of the wave tank has a glass wall 15 m in length. A rigid impermeable bottom of two different surface conditions, smooth and rough, was used. The slope of beach was 1/20 only. In case of the rough slope, the surface was uniformly roughened with spherical particles of 3 mm in diameter. The wave height was measured by using two wave gauges of capacitance type. One wave gauge was installed at a location in the region of uniform water depth to measure incident waves. The other gauge was installed at a point on the slope where two holes were opened to feed solid tracer particles slowly onto the bottom.

Polystyrene particles and glass balls with four different diameters were used as tracers. The properties of these particles are shown in Table 1. Polystyrene particles with a diameter of approximately 3 mm were coloured with paint. The glass balls were also coloured for each diameter.

Pairs of these tracer particles were simultaneously lifted up onto the sloping bottom through the two holes at a speed of 0.05 cm/sec by means of an apparatus devised by the authors. Fig. 1 shows this device of a constant speed feeder of tracer particles, which has three rods moved vertically by a small-sized variable speed motor. By the upward motion of the two short rods, tracer particles are lifted up and injected onto the bottom surface.

2.2 Experimental Procedure

Typical waves with three kinds of deepwater wave steepnesses were generated. Table 2 shows the characteristics of the waves and the water depth in the experiment.

Pairs of holes, through which the tracer particles were fed as mentioned before were made in the bottom plate at intervals of 40 cm in line with the direction of wave propagation. Movements of the polystyrene particles and glass balls, slowly pushed out on the bottom surface , were filmed by using a 16 mm movie camera (Bolex, H-16, EBM Electric) at a speed of about 24 frames/sec. Colour film was used to obtain informations from the coloured tracers. Trajectories of the particles moving on the bottom were traced from the film with the aid of a film motion analyzer (Motion Analyzer 160, NAC). To reduce the error caused by picture distortion, the particles were traced within the region of $\pm$ 10 cm from the center of each hole in the direction of wave propagation and within the region of $\pm$ 1.5 cm in the transverse direction. The error in reading the instantaneous location of tracers under these conditions was found to be about 3-4%. Transport distances of tracers during one wave cycle were divided by the wave period to obtain net transport velocities.

3. EXPERIMENTAL RESULTS AND DISCUSSIONS

3.1 Mass Transport Velocity on Bottom of Sloping Beach

Fig. 2 shows the mass transport velocity of polystyrene particles on the bottom of a roughened sloping beach with a nonlinear parameter of waves proposed by Goda(1983). In this figure, the dotted line denotes the theoretical values of the mass transport velocity at the edge of the bottom boundary layer by Longuet-Higgins i.e. $(5/4)\sinh^{-2}kh$. Symbols denote experimental data. A family of curves were determined by the

Table 1 Properties of tracer particles.

No.	Material	Mean Diameter (cm)	Fall Velocity (cm/sec)	Specific Gravity	Reynolds No. on Slope ($Vs \cdot d/\nu$)
1	Polystyrene	0.324	3.58	1.03	24
2	Glass	0.230	25.9	2.23	103
3	Glass	0.300	34.2	2.35	174
4	Glass	0.414	42.5	2.47	206
5	Glass	0.491	48.4	2.49	392

Table 2 Experimental conditions.

(a) in case of smooth slope

Wave Height H_o (cm)	Wave Period T (sec)	Depth (uniform) h_o (cm)	Depth (on slope) h (cm)	Wave Steepness H_o/L_o	Slope
2.73 ~ 3.02	1.68 ~ 1.70	40.0	1.90 ~ 30.5	0.006 ~ 0.007	1/20
5.97 ~ 6.88	1.41 ~ 1.43	40.0	1.90 ~ 30.5	0.021 ~ 0.024	1/20
8.09 ~ 8.94	1.10 ~ 1.12	40.0	1.90 ~ 30.5	0.046 ~ 0.050	1/20

(b) in case of roughened slope

Wave Height H_o (cm)	Wave Period T (sec)	Depth (uniform) h_o (cm)	Depth (on slope) h (cm)	Wave Steepness H_o/L_o	Slope
2.80 ~ 3.26	1.66 ~ 1.70	40.0	0.0 ~ 29.2	0.006 ~ 0.007	1/20
6.42 ~ 7.04	1.40 ~ 1.44	40.0	0.0 ~ 29.2	0.021 ~ 0.022	1/20
9.16 ~ 9.72	1.10 ~ 1.14	40.0	0.0 ~ 29.2	0.047 ~ 0.050	1/20

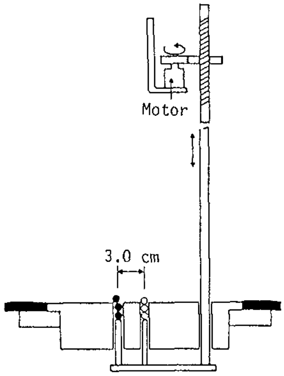

Fig. 1 Equipment for feeding tracer particles.

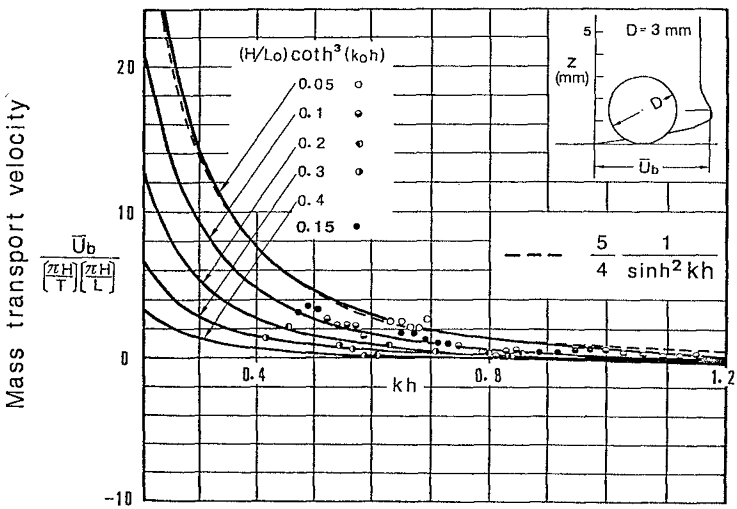

Fig. 2 Mass transport velocity of water on bottom of a sloping beach with a nonlinear parameter of waves proposed by Goda(1983).

method of least squares on the basis of the experimental data.

According to the paper by Goda(1983), the larger the value of the nonlinear parameter becomes, the more the nonlinearity of waves becomes remarkable. It is shown in Fig. 2 that the mass transport velocity on the bottom becomes small with an increase in the value of this parameter. In this connection, it is said that the mass transport velocity on the bottom of a sloping beach becomes small with an increase in the nonlinearity of waves.

3.2 Relationship between Mass Transport Velocity and Net Transport Velocity of Glass Balls

Figs. 3(a) and (b) show the relationships between the mass transport velocity and the net transport velocity of glass balls on a roughened beach of 1/20 slope. Assuming that the relationship is linear, it is expressed as follows:

$$(\bar{U}b/\sqrt{gHo})g = a(\bar{U}b/\sqrt{gHo})p + b \qquad (1)$$

in which $(\bar{U}b/\sqrt{gHo})g$ denotes the non-dimensional net transport velocity of glass balls and $(\bar{U}b/\sqrt{gHo})p$ that of the polystyrene particle, and both a and b are constants. The values of a and b in case of the roughened beach of 1/20 slope are listed in Table 3 and Table 4, in which ks denotes the roughness height (3mm), and D the diameter of a glass ball.

Table 3

Values of best-fit parameters a and b in the region of Fig. 3(a).

k_s/D	a	b
1.30	0.68	2.35
1.00	0.41	1.25
0.73	0.27	0.94
0.61	0.50	1.65
0.00*	0.56	0.50

Table 4

Values of best-fit parameters a and b in the region of Fig. 3(b).

k_s/D	a	b
1.30	1.42	0.06
1.00	0.68	0.79
0.73	0.24	0.92
0.61	0.28	0.40
0.00*	0.67	2.05

* : Data on a smooth sloping beach.

In the region offshore from the breaking point, the value of a becomes large with an increase in ks/D. In the surf zone, a does not change so much as in the offshore region.

3.3 Spatial Distribution of Net Transport Velocity of Glass Balls

Figs. 4(a) and (b) show the spatial distributions of the net transport velocity of glass balls with a parameter of ks/D. In these figures, the abscissa is the ratio of still water depth on the slope to

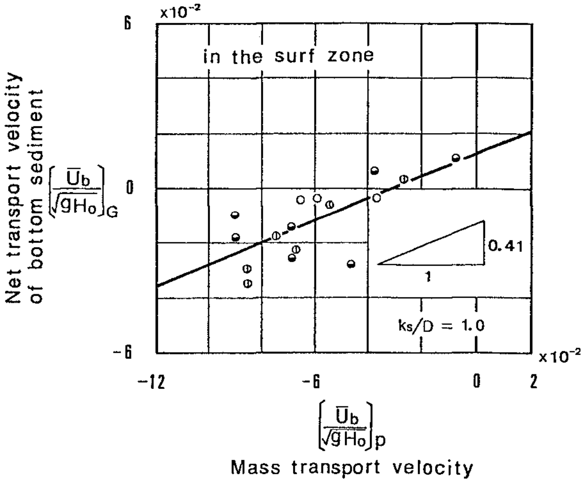

(a) in the surf zone

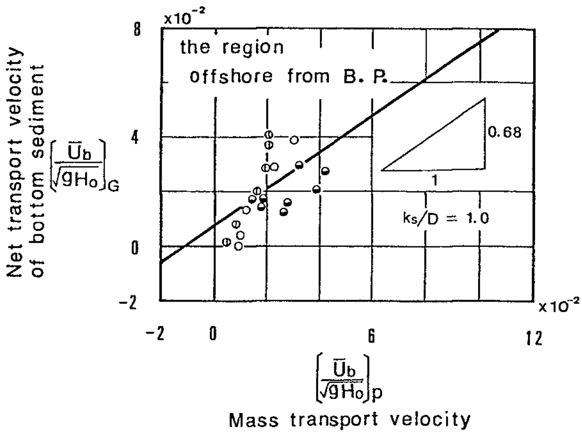

(b) in the region offshore from Breaking point

Fig. 3 Relationship between mass transport velocity and net transport velocity of glass balls (H_o/L_o: ○ 0.007, ⦶ 0.022, ● 0.049).

that at the breaking point, and the ordinate is the non-dimensional net transport velocity of glass balls. The positive component of $(\overline{U}b/\sqrt{gHo})g$ indicates the onshore transport . The data on a smooth sloping beach are plotted for reference.

From Fig. 4 , it is shown that firstly, the position where $(\overline{U}b/\sqrt{gHo})g$ becomes zero appears at three or four locations in case of the roughened slope, and at two locations in case of the smooth slope. Secondly, a dynamic equilibrium point near the plunging point of breaking waves where h/hb is 0.6-1.1 appears independently of both the bottom surface condition, smooth or rough, and the bottom sediment condition, relatively large or small to the bottom roughness. Thirdly, this dynamic equilibrium position corresponds to the place where sediment accumulates because the transport direction of bottom sediments offshore from this position is onshore and that onshore from this place is offshore. Fourthly, the position where the net transport velocity becomes zero in the offshore region has a qualitative difference due to the existence of roughness. That is to say, in case of the smooth surface, this position becomes a dynamic equilibrium point which corresponds to the "Null point" defined by Cornaglia(1889), Eagleson and Dean(1961), and other investigators. However, in case of the roughened surface, this position means a static place corresponding to a critical water depth for sediment movement.

3.4 Effect of Wave Steepness on Depth of Dynamic Equilibrium Point

Fig. 5 illustrates the effect of the deepwater wave steepness on the water depth in the dynamic equilibrium position. From this figure, two main points are found; the first is that the offshore equilibrium position appears in all cases of Ho/Lo, and the second is that the water depth of the offshore equilibrium position becomes shallow with a decrease in the deepwater wave steepness. On the other hand, the water depth in the onshore one is also affected by the deepwater wave steepness as well as in the offshore position.

4. MECHANISM OF ON-OFFSHORE SEDIMENT TRANSPORT

4.1 Discussions on Mechanism of Beach Profile Change

In this section, the mechanism of on-offshore transport of sediment as bed-load by wave action is discussed on the basis of the present experimental results. In addition, an attempt is made to explain the change of beach profile obtained in the existing experiment.

Considering the specific gravity of the tracers, it may be assumed that the net transport velocity of the polystyrene particles during a wave period closely apploximates the mass transport velocity of water, and that the velocity of the glass balls represents the net transport velocity of bottom sediments induced by wave action. As shown in Tables 3 and 4, there exists a clear correlation between the mass transport

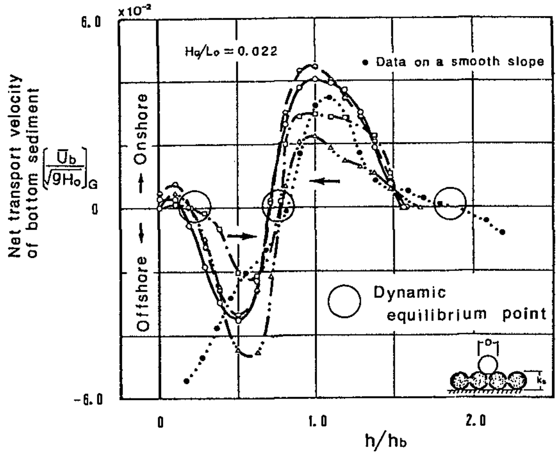

(a)

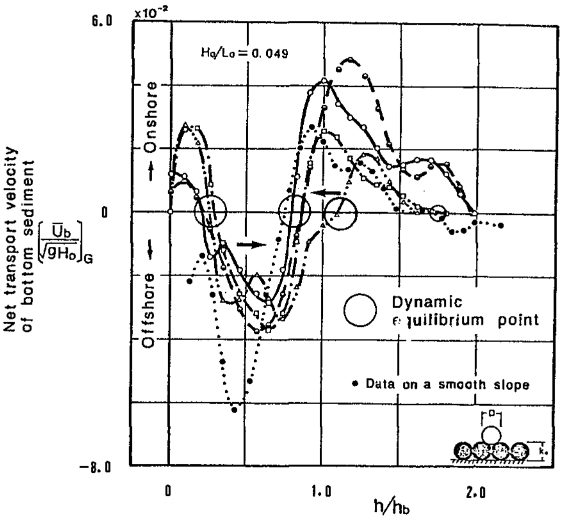

(b)

Fig. 4 Spatial distribution of net transport velocity of glass balls, $(\overline{U}b/\sqrt{gHo})_G$ (ks/D: ● 1.30, ○ 1.00, □ 0.73, △ 0.61).

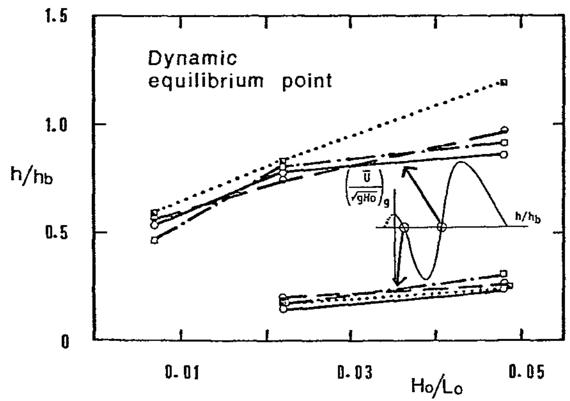

Fig. 5 Effect of deepwater wave steepness on water depth of dynamic equilibrium position (ks/D: ● 1.30, ○ 1.00, □ 0.73, △ 0.61).

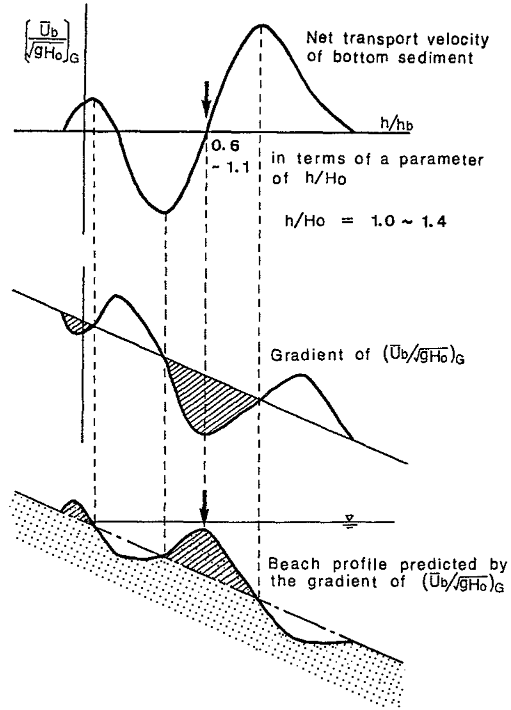

Fig. 6 Mechanism of beach profile deformation on basis of spatial distribution of net transport velocity of glass ball.

velocity of water near the bottom and the net transport velocity of the bottom sediments moving probably by rolling on a sloping bottom.

Here the mechanism of beach profile deformation is discussed on the basis of the spatial distribution of the net transport velocity of glass balls because the glass balls used in the present experiment have almost the same specific gravity as that of sand grains. Fundamental assumption in this model is that the bottom sediment is moved as bed-load.

Fig. 6 illustrates the mechanism of beach profile deformation on the basis of the spatial distribution of the net transport velocity of bottom sediments. The upper figure in Fig. 6 is the typical spatial distribution of the net transport velocity of sediments. This distribution is necessary to discuss the beach profile change, because the spatial difference of the net transport velocity of sediments causes beach profile deformation. The middle figure in Fig. 6 is the spatial distribution of the gradient of $(\overline{Ub}/\sqrt{gHo})g$. This gradient is directly related to the change of bottom profile configuration. The lowest figure in Fig. 6 is the beach profile predicted by the continuity relationship between the time variation of the bottom elevation and the spatial variation of the net transport rate of bottom sediments.

From the upper and the lowest figures in Fig. 6 , two points are found; the first is that the region offshore from the breaking point will be always eroded, and the second is that the offshore position of two dynamic equilibrium points represents the place where sediments accumulate. These two characteristics always appear in the beach profile evolution, independently of both the deepwater wave steepness (Ho/Lo) and the condition of bottom sediments (ks/D).

To elucidate the mechanism of sediment transport by wave action on a movable bed, an attempt is made to explain the process of beach profile change in model tests by considering the mass transport obtained for the spherical particles moving on a roughened slope. Beach deformation from an initial uniformly sloping beach to a final equilibrium profile can be classified into three types as shown in Fig.7 according to Sawaragi and Deguchi(1980). In Type I, accumulation occurs in the offshore region and erosion on the beach face, so that a bar is formed. In Type II, erosion occurs on the beach face and accumulation both on the back beach and in the offshore region, but the bottom in the region deeper than the place where the accumulation occurs in the offshore region has two different profiles, either accretive or erosive. In Type III, accumulation occurs on the beach face and erosion in the offshore region, so that a step is often formed.

The behaviour of the glass balls in the present experiment may correspond to that of coarse sediment transported as bed-load. As far as the present results are concerned, accumulation takes place near the location where the value of h/hb is 0.6-1.1, and the region offshore from the breaking point is eroded, independently of the deepwater wave steepness. Accordingly, when sediments are transported as bed-load, a uniformly sloping beach may probably change in the process of Type II-2 in Fig. 7 at the initial stage regardless of wave characteristics.

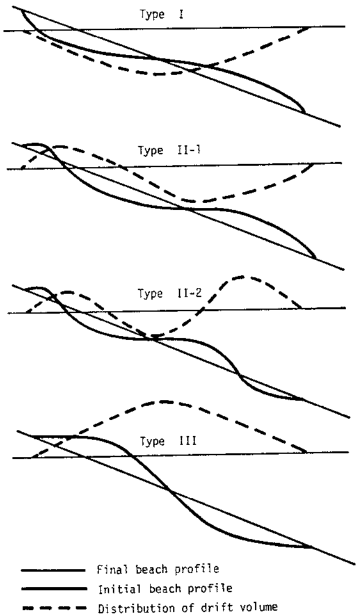

Fig. 7
Classification of beach process from uniformly sloping beach to equilibrium beach (Sawaragi and Deguchi, 1980).

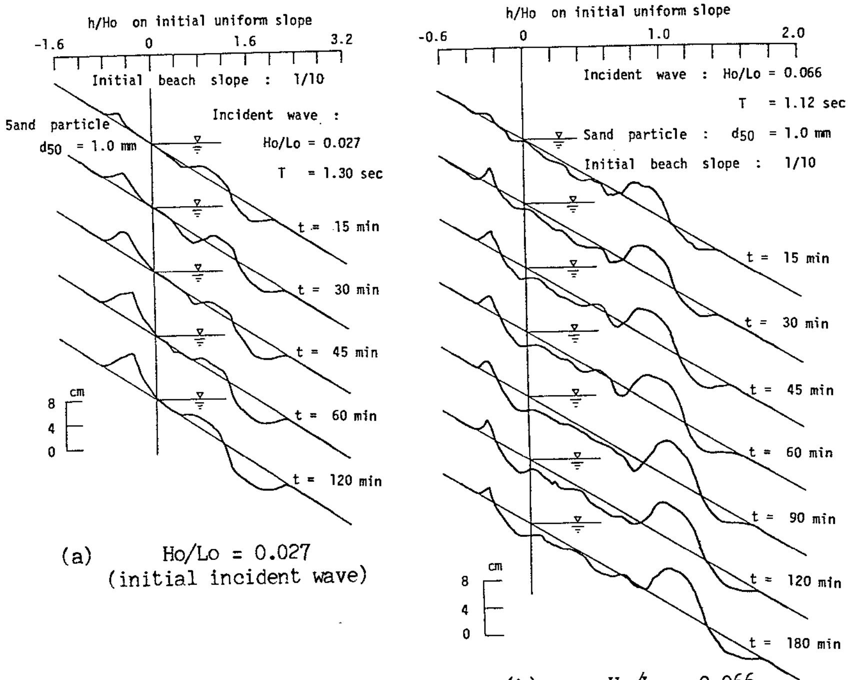

(a) $H_o/L_o = 0.027$
(initial incident wave)

(b) $H_o/L_o = 0.066$
(initial incident wave)

Fig. 8 Examples of beach profile deformation
(d_{50}= 1.0 mm, initial uniform slope: 1/10).

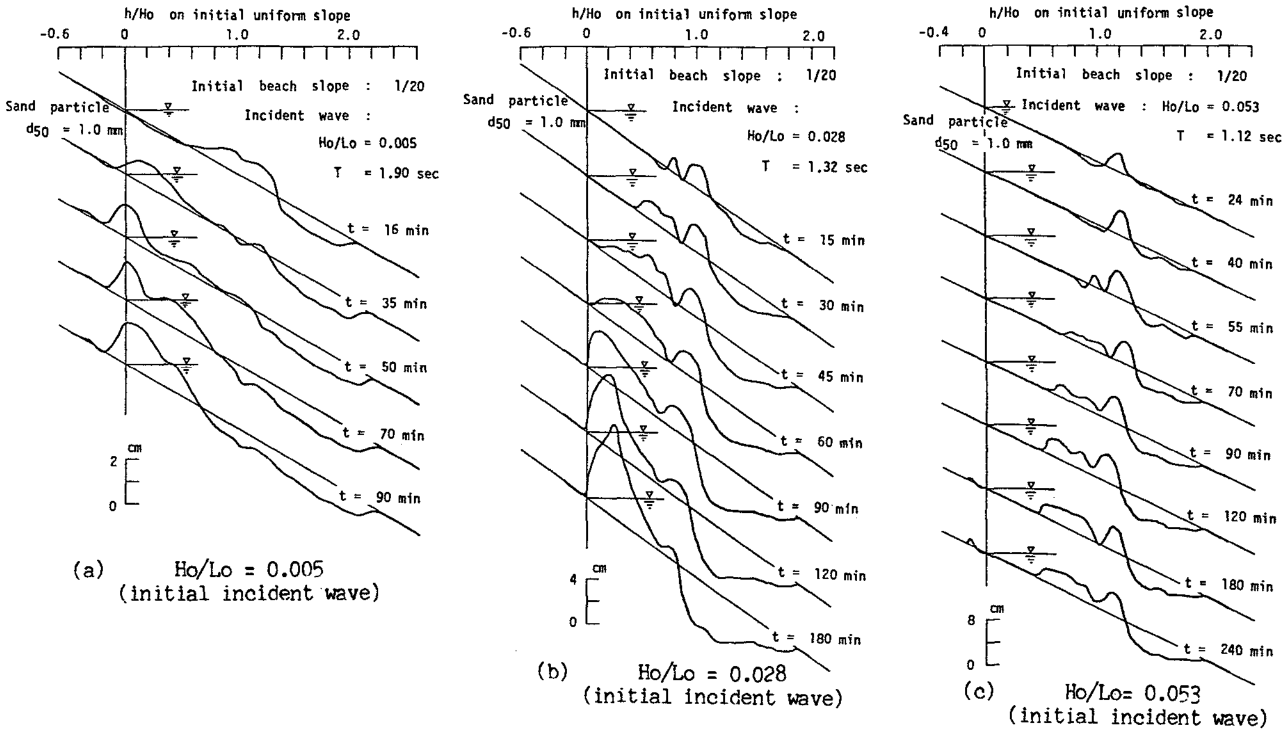

Fig. 9 Examples of beach profile deformation (d_{50}= 1.0 mm, initial uniform slope: 1/20).

On the other hand, when sediments are transported mainly in suspension, the beach profile is expected to change in the process of Type I or II-1, because the mass transport of water on a sloping beach is in the offshore direction in a middle layer above the bottom , and hence the suspended sediment is easily transported offshore. This explains the reason why fine sediments are easily transported offshore and form a large longshore bar.

4.2 Some Results of Model Beach Profile Deformation

In terms of a parameter of the still water depth to deepwater wave height ratio h/Ho, the region where h/hb is 0.6-1.1 corresponds to the region where h/Ho is 1.0-1.4.

Figs. 8 and 9 show some results of the beach profile deformation in case of initial uniform slopes 1/10 and 1/20 for each deepwater wave steepness. Sand of 1 mm in d_{50} was used in these movable bed tests in order to get the condition of bed-load movement of bottom sediments. To investigate the beach process in detail, the beach profile was measured at short time intervals.

From these results of movable bed tests under the same wave condition as in the fixed plane roughened beach, two main points are found; that is, the first is that a uniformly sloping beach with sand of relatively large diameter of 1 mm begins to change into the profile which has an accretive portion at the location where h/Ho is 1.0-1.2 at the initial stage. At the first stage toward an equilibrium state, this profile is formed in all cases, independently of both the deepwater wave steepness and the initial uniform slope. However, at the next stage, the beach profile changes under the influence of the wave steepness. The effect of the initial beach slope is seemed to be related to the speed of beach profile change, namely the deformation speed of the beach profile becomes rapid rather in case of 1/10 initial beach slope than in case of 1/20 initial beach slope. The second is that under the condition of bed-load movement of bottom sediment, in the process of the beach profile deformation the region offshore from the breaking point is always eroded independently of both Ho/Lo and the initial beach slope.

4.3 Discussions on Validity of Present Model

Fig. 10 shows the system of interactions among fluid characteristics, sediment movement and bottom configuration in the beach process. Each relationship clarified mainly in the unidirectional flow is briefly described as follows: relation (1) means the effect of the fluid field on the movement of bottom material, i.e. the fluid forces acting on the bottom sediments. In case of the wave field, the representatives in the relation (1) are considered to be the bottom shear stress, the mass transport velocity of water and the turbulenoe intensity by wave breaking. Relation (2) shows that for example, the von Karman constant diminishes as the concentration of suspended particles increases , Hino(1963). Relation (3) is the continuity condition of bottom sediment represented by the relation between the spatial gradient of the sediment transport rate and the time variation of the bottom elevation. Relation (4) means the effect of the gravity force on the sediment movement, that is to say, the on-offshore component of the gravity force of the bottom sediment becomes large with an increase in the slope of beach. Relation (5) shows that the fluid field is affected by the bottom configuration, i.e. the energy loss becomes different due to the bottom configuration. Relation (6) is not clear at present.

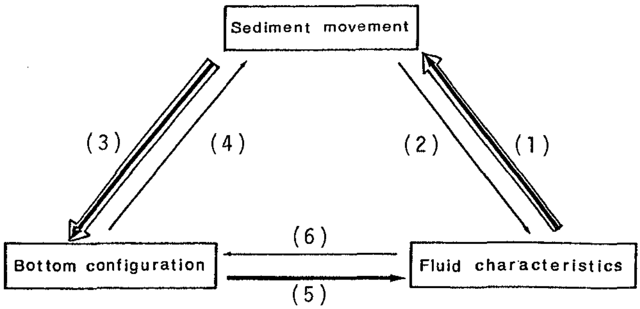

Fig. 10 System of interactions among fluid characteristics, sediment movement and bottom configuration.

From the results of the present investigation, when the sediment is transported as bed-load, the mechanism of beach profile deformation at the first stage from an initial uniform slope to an equilibrium state will be determined by the interaction between fluid characteristics and sediment movement and, therefore, can be explained on the basis of the spatial distribution of the net transport velocity of glass balls on a uniformly sloping beach.

However, at the second stage from a uniform slope to an equilibrium state, the mechanism of beach profile deformation will be governed by various interactions among fluid characteristics, sediment movement and bottom configuration.

5. CONCLUSIONS

In the limit of the present investigation, the following conclusions are drawn.

The mass transport velocity of water near the bottom on a roughened beach of 1/20 slope becomes small with an increase in the nonlinearity of waves.

The linearity between the mass transport velocity of water and the net transport velocity of bottom sediment is made clear by using tracers of polystyrene particle and glass balls.

When the sediment is transported as bed-load, the mechanism of beach profile deformation at the first stage from a uniform slope to an equilibrium state can be predicted on the basis of the spatial distribution of the net transport velocity of glass balls.

At the second stage from a uniform slope to an equilibrium state, the mechanism of sediment transport has to be investigated on the basis of hydraulic characteristics of flow fields for the deformed bottom configuration.

Under the condition of bed-load transport of sediment, in the process of the beach profile deformation, the region offshore from the breaking point is always eroded independently of both the deepwater wave steepness and the initial slope of a beach.

REFERENCES

Bijker, E.W., J.P.Th. Kalkwijk and T. Pieters: Mass transport in gravity waves on a sloping bottom, Proc. 14th Conf. Coastal Eng., 1974, pp. 447-465.

Cornaglia, P., this was translated for Benchmark volume by W.N. Felder, University of Virginia, from "Delle Spiaggie" in Accad. Naz. Lincei Atti Cl. Sci. Fis., Mat. e Nat. Mem. 5, ser. 4: 284-304 (1889), Benchmark Papers in Geology, Vol. 39, Dowden, Hutchinson and Ross, Inc., 1977, p. 382.

Eagleson, P.S. and R.G. Dean: Wave-induced motion of bottom sediment particles, Trans. ASCE, Vol. 126, Part 1, 1961, pp. 1162-1189.

Goda, Y.: A unified nonlinearity parameter of water waves, Report of the Port and Harbour Research Institute, Vol. 22, No. 3, 1983, pp. 3-30.

Hino, M.: Turbulent flow with suspended particles, Journal of the Hydraulics Division, ASCE, Vol. 89, No. HY4, Proc. Paper 3579, 1963, pp. 161-185.

Iwagaki, Y., W.-G. Pae and O. Moriguchi: Mechanism of sediment transport by waves on an impermeable slope, Coastal Eng. in Japan, Vol. 25, 1982, pp. 51-63.

Longuet-Higgins, M.S.: Mass transport in water waves, Phil. Trans. Roy. Soc. London, A, No. 903, Vol. 245, 1953, pp. 535-581.

Sawaragi, T. and I. Deguchi: On-offshore sediment transport rate in the surf zone, Proc. 17th Conf. Coastal Eng., 1980, pp. 1195-1214.

Stokes, G.G.: On the theory of oscillatory waves, Trans. Cambridge Phil. Soc., Vol. 8, 1847, pp. 441-455.

Wang, H.T., T. Sunamura and P.A. Hwang: Drift velocity at the wave breaking point, Coastal Eng., Vol. 6, No. 2, 1982, pp. 121-150.